

Optical constants for hard x-ray multilayers over the energy range $E = 35 - 180$ keV

D. L. Windt¹, S. Donguy¹, C. J. Hailey¹, J. Koglin¹,
V. Honkimaki², E. Ziegler², F. E. Christensen³, F. A. Harrison⁴

¹ *Columbia University, 550 West 120th St, New York, NY 10027*

² *European Synchrotron Radiation Facility, Grenoble, France*

³ *Danish Space Research Institute, Copenhagen, Denmark*

⁴ *California Institute of Technology, Pasadena, California*

ABSTRACT

We have determined experimentally optical constants for eight thin film materials that can be used in hard X-ray multilayer coatings. Thin film samples of Ni_{0.97}V_{0.03}, Mo, W, Pt, C, B₄C, Si and SiC were deposited by magnetron sputtering onto superpolished optical flats. Optical constants were determined from fits to reflectance-vs-incidence angle measurements made using synchrotron radiation over the energy range $E=35 - 180$ keV. We have also measured the X-ray reflectance of a prototype W/SiC multilayer coating over the energy range $E=35 - 100$ keV, and we compare the measured reflectance with a calculation using the newly derived optical constants.

1. INTRODUCTION

Depth-graded X-ray multilayer mirrors are the enabling technology for a new generation of astronomical space telescopes operating above $E=10$ keV, including the HEFT¹ and In-Focus² balloon instruments, and the Astro-G, Constellation-X, and XEUS satellite instruments.^{3,4} The multilayer coatings are designed to provide broad-band X-ray reflectance at grazing incidence. They are deposited onto light-weight cylindrical mirror substrates (such as thermally-formed glass⁵) which are then mounted into a highly-nested Wolter-type telescope geometry, thus providing sub-arcminute angular resolution and large effective area over a wide energy band.

The ability to produce optimized multilayer designs, and to reliably model instrument performance depends crucially on the availability of accurate optical constants for the constituent multilayer materials. Previously we measured the reflectance of prototype hard X-ray W/Si and W/SiC multilayers designed for use above 100 keV; we found that the measured reflectance did not agree well with calculations of the expected performance made using optical constants determined from theoretical atomic scattering factors and mass absorption coefficients. We were able to get better agreement however with calculations made using experimentally derived optical constants measured over the energy range $E = 120 - 180$ keV, which we determined for W and SiC, as well as for Ni_{0.93}V_{0.07} and B₄C.⁶ The discrepancy between the measured and theoretical optical constants can be partly attributed to incoherent (Compton) scattering, which is a particular concern especially for lighter elements at these energies, and which might not be properly accounted for in the available scattering factors and mass absorption coefficients.

As a consequence of the previous results just described, we have now made additional optical constants measurements, in order to characterize additional candidate multilayer materials, and to extend this optical data set to lower energies so as to benefit instruments currently under development. Specifically, the optical constants determined previously from $E=120 - 180$ keV for Ni_{0.97}V_{0.03}, W, B₄C, and SiC have now been complemented with new measurements from $E=35 - 120$ keV for these same materials, and in addition we have also measured the optical constants for Mo, Pt, C, and Si from $E=35 - 120$ keV. All the films were deposited onto superpolished optical flats by magnetron sputtering, using the deposition system described in §2. Optical constants were determined using the reflectance-vs-incidence-angle technique, described in §3. We present our results in §4, and our conclusions in §5.

2. FILM DEPOSITION

Single-layer films of order 300 Å in thickness of Ni_{0.97}V_{0.03}, Mo, W, Pt, C, B₄C, and SiC used to determine optical constants were deposited onto 5-cm-diameter super-polished glass substrates; a Si film was deposited onto a

super-polished sapphire substrate, in order to provide sufficient optical contrast in this case. With the exception of the Pt film, all coatings were prepared by planar DC magnetron sputtering using a deposition system that has been described previously.⁷ Only the Pt film was deposited using a small S-gun deposition system, also described previously.⁸

Our large planar magnetron system has recently been modified to allow for deposition in either the standard configuration, in which the magnetron cathodes are oriented horizontally and that is best suited for coating normal-incidence soft X-ray and EUV mirror substrates, or in a new ‘vertical’ configuration, which allows for more efficient deposition of depth-graded X-ray multilayers onto cylindrical mirror substrates. In the vertical configuration, illustrated in Fig.1, the 50-cm-long magnetron cathodes are mounted vertically, facing outward. Cylindrical mirror substrates are mounted in a cylindrical rack fixture and face inward. The substrate fixture is rotated past each cathode using a computer-controlled stepper-motor drive system, so that the thickness of an individual layer is determined precisely by the substrate velocity. The sputter gas (typically Ar) pressure is maintained using a closed-loop control system comprising a mass-flow controller and a capacitance manometer. The system is pumped with a cryopump and can reach a base pressure of $\sim 2 \times 10^{-8}$ Torr.

In order to characterize the coating thickness uniformity achievable on cylindrical mirror substrates using the

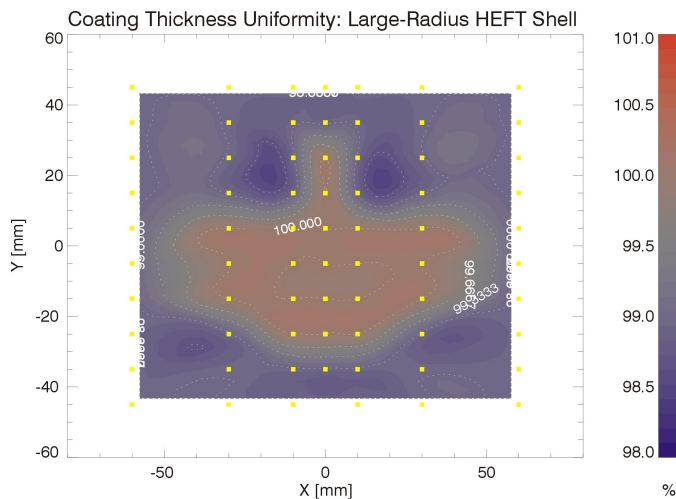


Figure 2. Multilayer coating thickness uniformity map obtained on a cylindrical mirror substrate having a radius of curvature of $R_c \sim 8$ cm. Coating thickness measurements were made at the positions of the yellow squares; smooth contours were drawn using bilinear spline interpolation between the measured points.

3. HARD X-RAY OPTICAL CONSTANT DETERMINATION

Hard X-ray reflectance measurements were made at beamline ID15A, at the European Synchrotron Radiation Facility. The experimental configuration is shown in Fig. 3. A bent, double-crystal Laue monochromator using Si (311) reflections was configured to scan either over the energy range from $E=35 - 120$ keV, or from $E=120 - 180$ keV. The monochromatic beam passed through two 130-mm-long W blocks separated by a $5 \mu\text{m}$ gap, thus providing

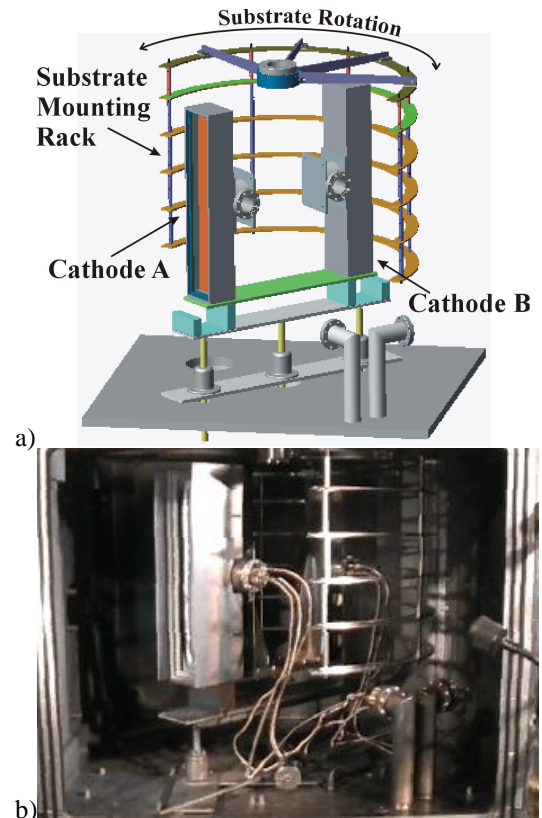


Figure 1. Schematic diagram (a) and photo (b) of the Columbia University magnetron sputtering system in the ‘vertical’ configuration, optimized for deposition onto cylindrical mirror substrates.

newly-configured deposition system shown in Fig. 1, thermally-formed glass substrates were coated with periodic multilayers, and the multilayer period was determined using normal-incidence soft X-ray reflectometry. A typical result is shown in Fig. 2. In this case, the variation in coating thickness across the surface of a cylindrical substrate measuring 10×12 cm, and having a radius of curvature of $R_c \sim 8$ cm, was found to be better than $\pm 0.75\%$.

collimation with $\delta\theta \sim 0.002^\circ$ divergence. A 2-circle diffractometer was constructed as follows: samples were placed on a precision rotation stage, and a Si PIN diode detector was mounted on a translation stage located 1.6 m from the sample; the translation stage was calibrated to act a “ 2θ ” rotation stage. The Si diode was used to measure the intensity of the straight-through and reflected beam. A second “ I_0 ” monitor detector was used to account for any drift in the incident flux, and the dark currents from both detectors were measured and subtracted from all intensity measurements. The absolute energy scale of the monochromator was determined by measuring the location of the Ta and Pb K-edges using foils of these materials for the low-energy configuration, or by measuring the angular position of the (111) reflection from an Al powder sample for the high-energy configuration.

Optical constants for the eight materials listed above were determined using the reflectance-vs-incidence-angle technique.⁹ Non-linear, least-square χ^2 minimization fits to the R- θ curves were performed using IMD, with the optical constants (1- n) and k set as fit parameters.

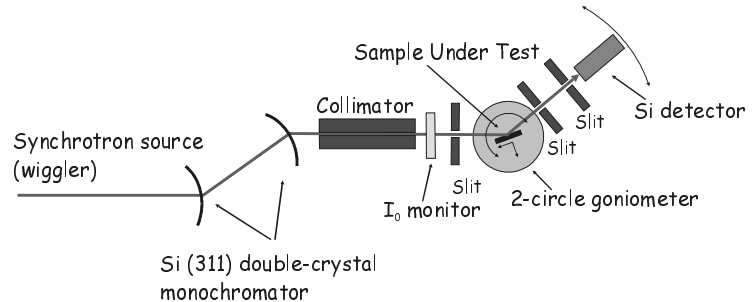


Figure 3. Experimental configuration at ESRF, beamline ID15A, used for hard X-ray reflectance measurements. The double-crystal monochromator is actually oriented in the horizontal plane, but for simplicity is shown here in the vertical plane.

4. RESULTS

The values of the optical constants (1- n) and k for the eight materials listed above, determined from fits to the hard X-ray reflectance data as just described, are plotted as symbols in Fig. 4; the dashed lines are smooth polynomial fits to the best-fit optical constants. The scatter in the best-fit optical constants (which illustrates the precision with which these data have been determined) is greatest for the k values, increases with increasing energy, and is greatest for the lighter elements. These trends are due principally to the fact that the derived value of k is strongly dependant on the measured position of the critical angle for total external reflection; the critical angle decreases with increasing energy and with decreasing density, and for the lighter elements at the higher energies, occurs close to the measurement limit imposed by the size of the incident beam and the size of the substrate, hence the greater experimental uncertainty under these conditions.

Shown also in Fig.4 as dotted lines are optical constants computed from a combination of theoretical atomic scattering factors¹⁰ that do not include incoherent scattering and theoretical mass absorption coefficients¹¹ that do include incoherent scattering. In this case, the optical constants were computed from the atomic scattering factors (f_1, f_2) in the usual way,¹² assuming bulk material densities ρ , but the values of the extinction coefficient k were simply replaced with those determined from the mass absorption coefficient, μ , according to $k = \mu\rho\lambda/4\pi$. These theoretical optical constants deviate significantly from the experimental data in all cases, but particularly for the lighter elements at higher energies.

Shown in Fig. 5 is the reflectance of a prototype W/SiC depth-graded multilayer, measured as a function of energy at a fixed incidence angle of 0.14 deg, using the experimental setup shown in Fig. 3. This film contains $N=250$ periods, with bilayer thicknesses ranging from $d_{\min}=26.1 \text{ \AA}$ to $d_{\max}=191.8 \text{ \AA}$. As expected, this multilayer reflects most efficiently at energies below the W K-edge ($E=69.5 \text{ keV}$).

Multilayer reflectance curves calculated using both theoretical optical constants (dashed line) as well as the new experimental optical constants (dotted line) are shown as well in Fig 5. Acceptable fits to the measured reflectance curve can be obtained with either data set, however the interface widths σ suggested by these fits differ: a calculation using theoretical optical constants suggests $\sigma=3.75 \text{ \AA}$, while the experimental optical constants suggest $\sigma=3.0 \text{ \AA}$, thus reflecting the greater absorption (i.e., larger k values) implicit in the experimental optical constants. Though not presented here, we found comparable results for a similar W/Si depth-graded multilayer measured over the same energy range. Although we have no independent measurement of the interface width over the range of spatial frequencies appropriate to these reflectance measurements that could be used to better gauge these two fits, it seems prudent nevertheless to use the experimental optical constants for future multilayer design and modeling activities.

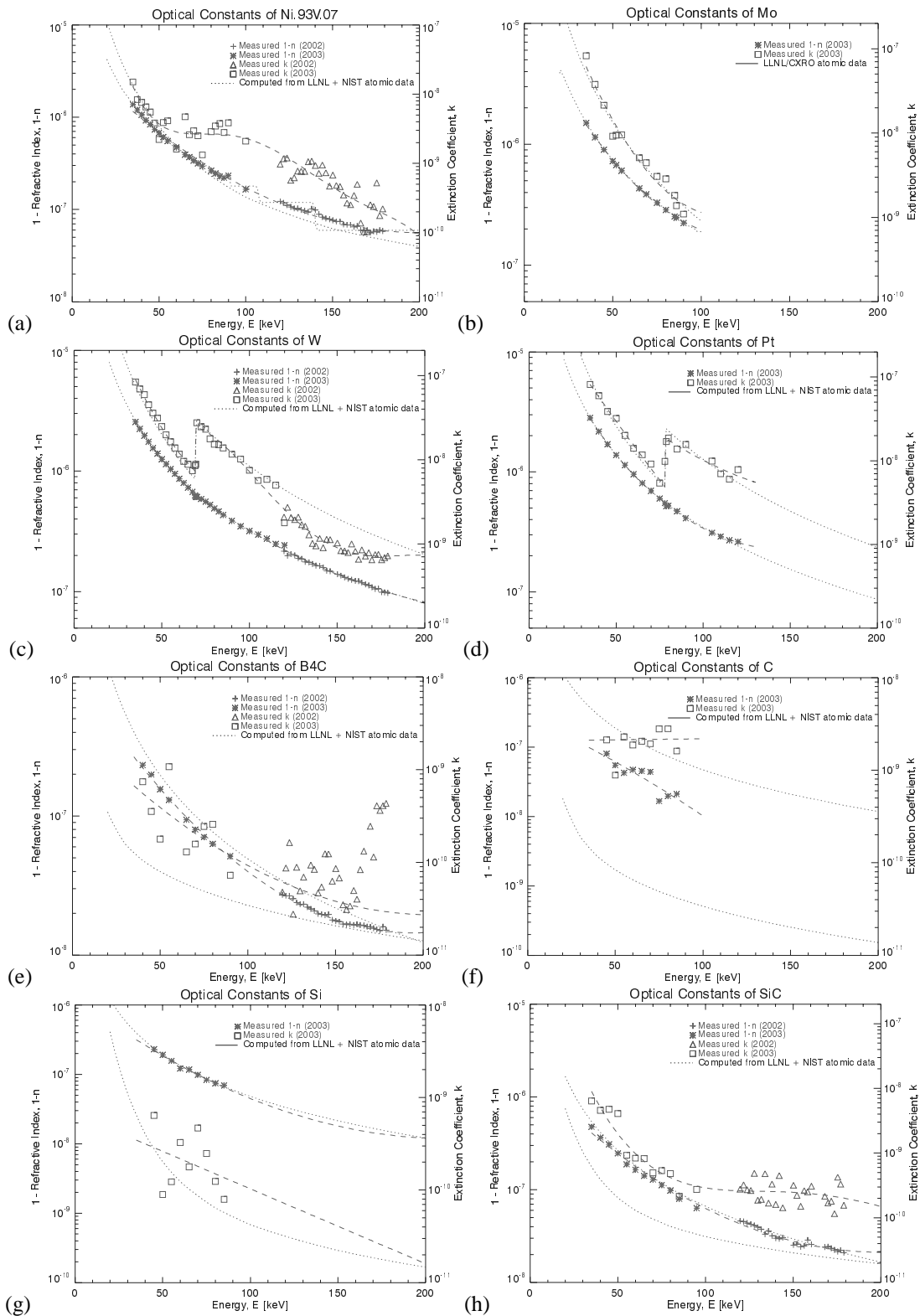


Figure 4. Optical constants ($1-n$) and k derived from reflectance-vs-incidence angle data for (a) $Ni_{.97}V_{.03}$, (b) Mo , (c) W , (d) Pt , (e) B_4C , (f) C , (g) Si and (h) SiC . Measurements made in 2003 in from 35 – 120 keV are plotted as stars ($1-n$) and squares (k), while measurements made in 2002 from 120 – 180 keV are plotted as crosses ($1-n$) and triangles (k). The dashed lines are polynomial fits to the experimental data. The dotted lines are theoretical values computed from atomic scattering factors and mass absorption coefficients, as described in the text.

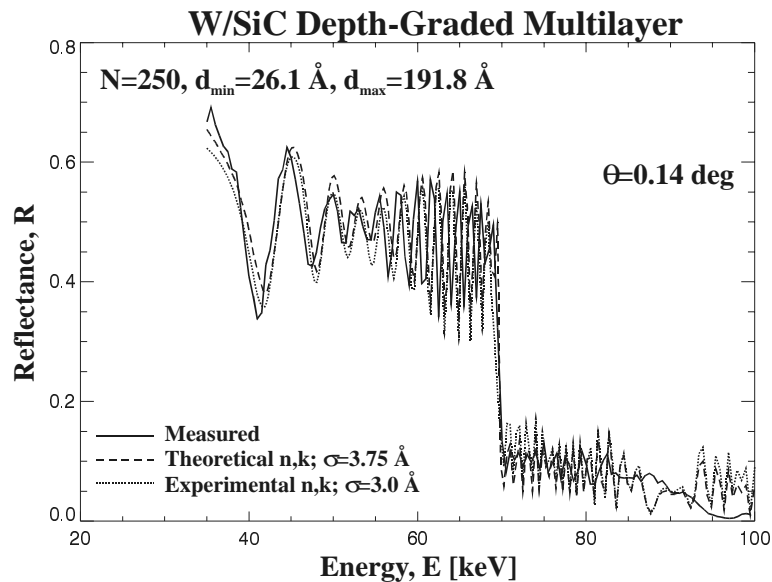


Figure 5. Reflectance of a depth-graded W/SiC multilayer containing $N=250$ bilayers as indicated. The solid curve is the measured reflectance; also shown is the reflectance calculated using theoretical optical constants (dashed line) and experimentally-derived optical constants (dotted line), using interface widths of $\sigma=3.75$ Å and $\sigma=3.0$ Å respectively.

5. CONCLUSIONS

We have measured the optical constants of eight candidate multilayer materials over the energy range $E=35 - 180$ keV. Thin films of $\text{Ni}_{.97}\text{V}_{.03}$, Mo, W, Pt, C, B_4C , Si and SiC were deposited onto superpolished optical flats, using a magnetron sputtering system optimized for depth-graded multilayer deposition onto cylindrical mirror substrates. Reflectance-vs-incidence angle measurements were made using synchrotron radiation, and non-linear, least-squares fits to the reflectance data were used to derive optical constants.

We find that the measured optical constants deviate significantly from optical constants determined from theoretical atomic scattering factors and mass absorption coefficients, particularly for lighter materials at higher energies where incoherent scattering is most important. We also found that the new experimental optical constants for W, Si and SiC can be used to accurately model the reflectance of depth-graded multilayers comprising these materials. We expect similar results will be obtained if the new optical constant data are used to model the performance of other multilayers comprising any of the other materials described here.

ACKNOWLEDGEMENTS

This research was sponsored in part by a grant from NASA.

REFERENCES

- ¹ F. A. Harrison, S. E. Boggs, A. Bolotnikov, F. E. Christensen, W. R. Cook, W. W. Craig, C. J. Hailey, M. Jimenez-Garate, P. H. Mao, S. E. Schindler, and D. L. Windt, *Proc. SPIE*, 4012, 696 (2000)
- ² K. Yamashita, P. J. Serlemitsos, J. Tueller, S. D. Barthelmy, L. M. Bartlett, K. W. Chan, A. Furuzawa, N. Gehrels, K. Haga, H. Kunieda, P. Kurczynski, G. Lodha, N. Nakajo, N. Nakamura, Y. Namba, Y. Okajima, D. Palmer, A. Parsons, Y. Soong, S. M. Stahl, H. Takata, K. Tamura, Y. Tawara, and B. J. Teegarden, *App. Opt.* 37, 8067 (1998)
- ³ H. Tananbaum, N. White, and P. Sullivan, eds. '*Proceedings of the High Throughput X-Ray Spectroscopy Workshop*', Harvard-Smithsonian Center for Astrophysics, Cambridge, MA (1996)
- ⁴ D. Lumb, M. Bavdaz, A. J. Peacock, *Proc. SPIE* 5165 (#5165-01)

⁵ See, for example, J. Koglin *et al*, these proceedings (#5168-12).

⁶ D. L. Windt, S. Donguy, C. J. Hailey, J. Koglin, V. Honkimaki, E. Ziegler, F. E. Christensen, C. M. H. Chen, F. A. Harrison, W. W. Craig, *App. Opt.*, 42, 2415 – 2421 (2003)

⁷ D. L. Windt and W. K. Waskiewicz, *J. Vac. Sci. Technol. B*, 12, 3826 (1994)

⁸ D. L. Windt, J. Dalla Torre, G. H. Gilmer, J. Sapjeta, R. Kalyanaraman, F. H. Baumann, P. L. O'Sullivan, D. Dunn, R. Hull, *Proc. MRS*, 564, 307 – 312 (1999)

⁹ D. L. Windt, W. Cash, M. Scott, P. Arendt, B. Newnam, R. F. Fisher, A. B. Swartzlander, M. Pinneo, and P. Z. Takacs, *Appl. Op.*, 27, 279-295 (1988)

¹⁰ High-energy atomic scattering factors are available at <<http://www-phys.llnl.gov/Research/scattering/asf.html>>

¹¹ High-energy mass absorption coefficients are available for elements at <<http://physics.nist.gov/PhysRefData/XrayMassCoef/cover.html>>, and for compounds at <<http://bnlnd2.dne.bnl.gov/>>.

¹² B. L. Henke, E. M. Gullikson, and J. C. Davis, *At. Data Nuclear Data Tables*, 54, 181 (1993)